

# Implementing fully relativistic hydrodynamics in three dimensions

T. W. Baumgarte<sup>1</sup>, S. A. Hughes<sup>1</sup>, L. Rezzolla<sup>1</sup>, S. L. Shapiro<sup>1,2</sup> and M. Shibata<sup>1,3</sup>

<sup>1</sup>*Department of Physics, University of Illinois at Urbana-Champaign, Urbana, IL 61801*

<sup>2</sup>*Department of Astronomy and NCSA, University of Illinois at Urbana-Champaign, Urbana, IL 61801*

<sup>3</sup>*Department of Earth and Space Science, Osaka University, Toyonaka, Osaka 560-0043, Japan*

**Abstract.** We report on our numerical implementation of fully relativistic hydrodynamics coupled to Einstein’s field equations in three spatial dimensions. We briefly review several steps in our code development, including our recasting of Einstein’s equations and several tests which demonstrate its advantages for numerical integrations. We outline our implementation of relativistic hydrodynamics, and present numerical results for the evolution of both stable and unstable Oppenheimer-Volkov equilibrium stars, which represent a very promising first test of our code.

## INTRODUCTION

The physics of compact objects is entering a particularly exciting phase. New instruments, including X-Ray and Gamma-Ray satellites and the new neutrino observatories SNO and Super-Kamiokande, can now yield unprecedented observations of neutron stars and black holes. Perhaps most excitingly, the new gravitational wave detectors LIGO, TAMA, GEO and VIRGO promise to open a gravitational wave window to the Universe and make gravitational wave astronomy a reality (see, e.g., [1]).

Simultaneously, the availability of computational resources at modern supercomputers makes the simulation of realistic astrophysical scenarios involving relativistic compact objects feasible. Several groups, including two “Grand Challenge Alliances” [2], have launched efforts to construct numerical codes capable of solving Einstein’s equations with or without matter sources in three dimensions, and simulating the merger of black hole or neutron star binaries (see, e.g., [3–9]). Numerical simulations will be necessary to predict the gravitational wave form from such processes to increase the likelihood of detections and, ultimately, to extract physical information from observations. Even though much progress has recently been made (see [9] for the most recent developments), significant obstacles still remain.

In this contribution, we report on our systematic approach towards constructing such a numerical code. We first review our formulation of Einstein’s equations and describe several tests, both for vacuum spacetimes and analytical matter sources, which demonstrate its advantages for numerical integrations. We then outline our implementation of hydrodynamics, and present promising numerical test results. We adopt geometrized units ( $G = c = 1$ ) and the convention that Greek indices run from 0 to 3, while Latin indices only run from 1 to 3.

## EVOLUTION OF THE GRAVITATIONAL FIELDS

Most numerical implementations of Einstein’s equations adopt a Cauchy formulation based on the 3+1 formulation by Arnowitt, Deser and Misner ([10], see, e.g., [11] for an alternative characteristic formulation). However, a straightforward implementation of these “undressed” ADM equations tends to develop instabilities even for the evolution of small amplitude gravitational waves on a flat background (compare [12]). Following Shibata and Nakamura [13] and the spirit of many earlier one and two-dimensional codes [14], we have recently developed a modification of the ADM equations which proves to be much more suitable for numerical implementations [15].

More specifically, we modify the ADM equations in two ways. First, we split the spatial metric  $\gamma_{ij}$  into a conformal factor  $\exp(\phi)$  and a conformally related metric  $\tilde{\gamma}_{ij}$  according to

$$\gamma_{ij} = e^{4\phi} \tilde{\gamma}_{ij} \tag{1}$$

and evolve  $\phi$  and  $\tilde{\gamma}_{ij}$  separately. We choose  $\phi$  such that  $\det(\tilde{\gamma}_{ij}) = 1$ , and similarly split the extrinsic curvature into its trace and its trace-free part. This split separates the “radiative” variables from the “non-radiative” variables in the spirit of the “York-Lichnerowicz” decomposition [16].

In the second stage we introduce “conformal connection functions”

$$\tilde{\Gamma}^i \equiv \tilde{\gamma}^{lm} \tilde{\Gamma}_{lm}^i = -\tilde{\gamma}^{il}{}_{,l} \quad (2)$$

as independent functions (compare [17]). Some of the mixed second derivatives of  $\tilde{\gamma}_{ij}$  in the conformal, spatial Ricci tensor  $\tilde{R}_{ij}$  can now be written as first derivatives of the  $\tilde{\Gamma}^i$ . As a result,  $\tilde{R}_{ij}$  becomes a manifestly elliptic operator on the metric  $\tilde{\gamma}_{ij}$ . The analogous technique was used for the four-dimensional Ricci tensor  $R_{\alpha\beta}$  as early as in the 1920’s to make Einstein’s equations manifestly hyperbolic [18]. For more details of our formulation, including an evolution equation for the  $\tilde{\Gamma}^i$ , the reader is referred to [15] (see also the mathematical analysis in [19], and further numerical applications in [20]).

In [15], we tested this form of Einstein’s equations for small amplitude gravitational waves, and found that it performs far better than a similar implementation of the original ADM formulation. In particular, we found that we could evolve such waves with harmonic slicing without encountering growing instabilities, whereas the original ADM code crashed after about 35 light-crossing times for the same initial data. In [21], we inserted analytic matter sources on the right hand side of Einstein’s equations and evolved the fields in their presence. This approach allows us to study the numerical properties of the field evolution in the presence of highly relativistic matter sources without having to solve the equations of hydrodynamics: “hydro-without-hydro”. We inserted the Oppenheimer-Snyder solution for a relativistic, static star to test the long term stability of the evolution code, and the Oppenheimer-Volkov solution for the collapse of a sphere of dust to a Schwarzschild black hole. These simulations focus on the highly relativistic, longitudinal fields, and complement our earlier tests involving dynamical transverse fields in [15]. With the code having passed these tests, we are now implementing both collisionless matter, which will be described elsewhere, and hydrodynamics, as described below, to evolve the matter self-consistently with the fields.

## RELATIVISTIC HYDRODYNAMICS

For a perfect fluid, the stress-energy tensor can be written

$$T^{\alpha\beta} = (\rho_0 + \rho_0\epsilon + P)u^\alpha u^\beta + P g^{\alpha\beta}, \quad (3)$$

where  $\rho_0$  is the rest mass density,  $\epsilon$  the specific internal density,  $P$  the pressure,  $u^\alpha$  the fluid four velocity, and  $g_{\alpha\beta}$  the four dimensional spacetime metric. We construct constant entropy initial data with a polytropic equation of state

$$P = K \rho_0^\Gamma, \quad (4)$$

where  $\Gamma = 1 + 1/n$  and  $n$  is the polytropic index, and where we assume the polytropic constant  $K$  to be unity without loss of generality. During the evolution, we adopt the gamma-law relation appropriate for adiabatic flow,

$$P = (\Gamma - 1)\rho_0\epsilon. \quad (5)$$

Following [9,22], we write the equation of continuity

$$(\rho_0 u^\alpha)_{;\alpha} = 0 \quad (6)$$

and the equations of motion

$$T^{\alpha\beta}{}_{;\beta} = 0 \quad (7)$$

in the form

$$\rho_{*,t} + (\rho_* v^i)_{,i} = 0, \quad (8)$$

$$e_{*,t} + (e_* v^i)_{,i} = 0, \quad (9)$$

$$\begin{aligned} (\rho_* \tilde{u}_i)_{,t} + (\rho_* \tilde{u}_i v^j)_{,j} = & -\alpha e^{6\phi} P_{,i} - \alpha \rho_* \tilde{u}^0 \alpha_{,i} + \rho_* \tilde{u}_l \beta^l{}_{,i} + \\ & \frac{\rho_* \tilde{u}_l \tilde{u}_m}{e^{4\phi} \tilde{u}^0} \left( 2\tilde{\gamma}^{lm} \phi_{,i} + \frac{1}{2} \left( \tilde{\Gamma}_{ki}^l \tilde{\gamma}^{km} + \tilde{\Gamma}_{ki}^m \tilde{\gamma}^{kl} \right) \right). \end{aligned} \quad (10)$$

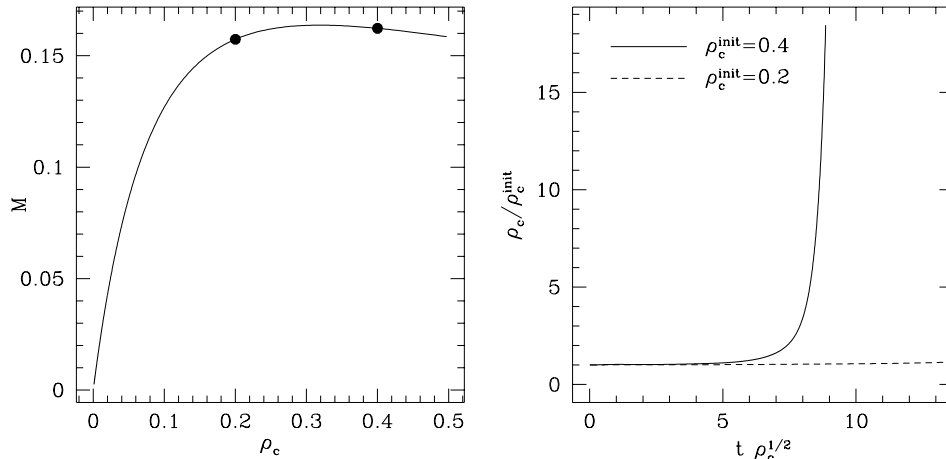


**FIGURE 1.** Mass versus central density for a  $n = 1$  polytrope (left panel). We chose the two configurations marked by the filled circles ( $\rho_c = 0.2$  and  $\rho_c = 0.4$ ) as initial data for our dynamical simulations. The central density as a function of time for the evolution of the two initial data sets (right panel). As expected, the  $\rho_c = 0.4$  configuration soon collapses, whereas the  $\rho_c = 0.2$  configuration remains stable for several dynamical timescales.

Here we have defined the auxiliary quantities

$$\rho_* \equiv \alpha e^{6\phi} u^0 \rho_0, \quad (11)$$

$$e_* \equiv \alpha e^{6\phi} u^0 (\rho_0 \epsilon)^{1/\Gamma}, \quad (12)$$

$$\tilde{u}_i \equiv (1 + \Gamma \epsilon) u_i, \quad (13)$$

$$\tilde{u}^0 \equiv (1 + \Gamma \epsilon) u^0, \quad (14)$$

$$v^i \equiv u^i / u^0 = -\beta^i + \gamma^{ij} u_j / u^0. \quad (15)$$

Similar equations have been used by many other groups (e.g. [23] and references therein). We integrate equations (8) - (10) with an artificial viscosity scheme suggested in [3] (see [8] for implementations of more elaborate shock capturing schemes). Given  $\rho_*$ ,  $e_*$  and  $\tilde{u}_i$  on a new timelevel,  $u^0$  can be found iteratively from the normalization relation  $u^\alpha u_\alpha = -1$ , which yields

$$(\alpha u^0)^2 = 1 + \frac{\tilde{\gamma}^{ij} \tilde{u}_i \tilde{u}_j}{e^{4\phi}} \left( 1 + \Gamma \frac{e_*^\Gamma}{\rho_* (\alpha u^0 e^{6\phi})^{\Gamma-1}} \right)^{-2}. \quad (16)$$

The matter sources for the right hand sides of Einstein's equations can then be constructed from these variables.

## NUMERICAL RESULTS

As a first test of our implementation of hydrodynamics, we adopt the Oppenheimer-Volkov solution describing equilibrium neutron stars in spherical symmetry as initial data and evolve these dynamically. Constructing a sequence of such Oppenheimer-Volkov solutions for increasing central rest mass densities  $\rho_c$ , the ADM mass  $M$  of the star takes a maximum  $M_{\max}$  at  $\rho_c^{\text{crit}}$  (see the left panel in Figure 1). For central densities smaller than  $\rho_c^{\text{crit}}$ , the star is in stable equilibrium, while for  $\rho_c > \rho_c^{\text{crit}}$  it is unstable and will collapse to a black hole.

We adopt a polytropic equation of state with  $\Gamma = 2$  ( $n = 1$ ), for which  $\rho_c^{\text{crit}} = 0.32$  and  $M_{\max} = 0.164$  when  $K = 1$ . We choose as initial data the two configurations marked with filled circles in Figure 1; a stable configuration with  $\rho_c = 0.2$ ,  $M = 0.157$  and  $R/M = 5.5$ , and an unstable configuration with  $\rho_c = 0.4$ ,  $M = 0.162$  and  $R/M = 4.4$ .

In the right panel of Figure 1, we show the central density as a function of time for the two initial configurations. We performed these runs on quite modest numerical grids with  $(64)^3$  gridpoints using cartesian coordinates and imposing outgoing wave boundary conditions at  $x, y, z = 2$ . We employ harmonic slicing and zero shift. As expected, the unstable configuration soon collapses, while the stable configuration remains stable for several dynamical timescales (the period of the fundamental radial oscillation for a  $\rho_c = 0.2$  configuration is approximately  $7\rho_c^{-1/2}$ , compare [9]). Ultimately, accumulation of numerical error causes this configuration to collapse too, but this can be delayed by increasing the grid resolution.

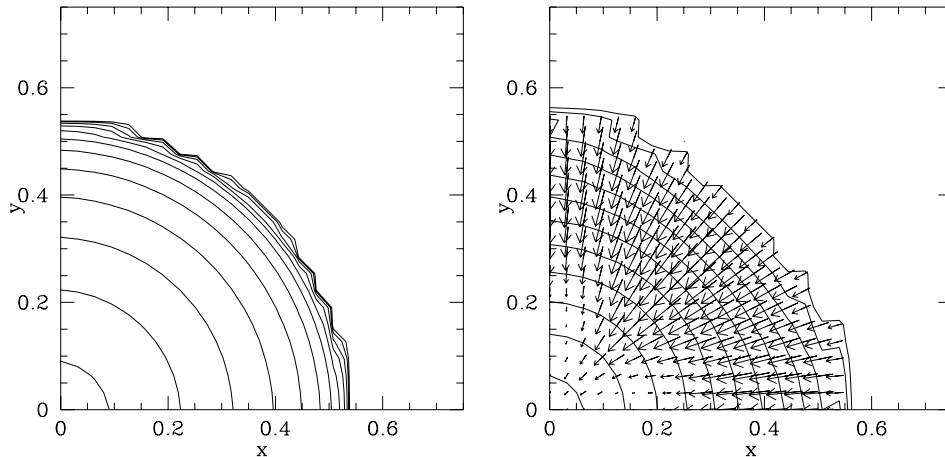


**FIGURE 2.** Rest mass density contours at  $t = 0$  (left panel) and  $t = 13$  (right panel) in the  $z = 0$  (equatorial) plane for the unstable configuration with  $\rho_c = 0.4$  initially. The contours logarithmically span densities between  $\rho_c$  and  $10^{-3}\rho_c$ . We also include arrows indicating the fluid flow  $\tilde{u}_i$ .

In Figure 2 we show density contours at the beginning and towards the end of the simulation for the unstable configuration with  $\rho_c = 0.4$  initially. We also include arrows indicating the fluid flow  $\tilde{u}_i$ . The star is rapidly contracting and collapsing to a black hole. Up to the late stage of the collapse, the mass  $M$  is conserved to about 5%. We can follow the collapse to about a 18 fold increase of the central density. By this time, the central lapse has decreased from 0.4 initially to about 0.03.

## SUMMARY AND DISCUSSION

We report on our systematic approach towards constructing a fully relativistic hydrodynamics code in three spatial dimensions. As part of this program, we have developed a new formulation of Einstein’s equations which in several tests and applications has proved to be much more suitable for numerical implementations than the traditional ADM formulation [15,20]. Mathematical properties of this formulation have been analyzed in [19]. We have studied the evolution of small amplitude gravitational waves to test dynamical transverse fields and have inserted analytical solutions as matter sources (hydro-without-hydro) to test highly relativistic longitudinal fields.

We outline our implementation of the relativistic equations of hydrodynamics and present preliminary test results for spherical neutron stars in hydrostatic equilibrium (Oppenheimer-Volkov stars). As expected, we find that stable stars remain stable for several dynamical timescales, while unstable stars soon collapse to black holes. We conclude that our method seems like a very promising approach towards simulating the final plunge and merger of binary neutron stars.

On a more speculative note, we point out that fully self-consistent hydrodynamics may not be a feasible approach towards simulating the coalescence and gravitational wave emission from neutron stars in the intermediate inspiral phase. In this epoch, the stars are very close and interact through a strongly relativistic tidal field, but reside outside the innermost stable circular orbit and hence move on a nearly circular orbit. Simulating the slow inspiral would require evolving the stars for hundreds or thousands of orbits, which is presently impossible. It may be possible, however, to insert known quasi-equilibrium binary configurations (e.g. [6,7]) into the field evolution code to get the transverse wave components approximately. Decreasing the orbital separation (and increasing the binding energy) at the rate consistent with the computed outflow of gravitational-wave energy would generate an approximate strong-field wave inspiral pattern. Such a “hydro-without-hydro” calculation may yield an approximate gravitational waveform from inspiraling neutron stars, without having to couple the matter and field integrations.

Calculations were performed on SGI CRAY Origin2000 computer systems at the National Center for Supercomputing Applications, University of Illinois at Urbana-Champaign. This work was supported by NSF Grants AST 96-18524 and PHY 99-02833 and NASA Grant NAG 5-7152 at Illinois.

## REFERENCES

1. See article by P. Saulson in this Volume.
2. Information about the Binary Black Hole Grand Challenge can be found at [www.npac.syr.edu/projects/bh/](http://www.npac.syr.edu/projects/bh/), and about the Binary Neutron Star Grand Challenge at [wugrav.wustl.edu/Relativ/nsgc.html](http://wugrav.wustl.edu/Relativ/nsgc.html).
3. K. Oohara and T. Nakamura, *Prog. Theor. Phys.* **82**, 535 (1989).
4. K. Oohara and T. Nakamura, in *Relativistic Gravitation and Gravitational Radiation*, edited by J.-A. Marck and J.-P. Lasota (Cambridge University Press, Cambridge, 1997).
5. J. R. Wilson and G. J. Mathews, *Phys. Rev. Lett.* **75**, 4161 (1995); J. R. Wilson, G. J. Mathews and P. Marronetti, *Phys. Rev. D* **54**, 1317 (1996).
6. T. W. Baumgarte, G. B. Cook, M. A. Scheel, S. L. Shapiro, and S. A. Teukolsky, *Phys. Rev. Lett.* **79**, 1182 (1997); *Phys. Rev. D* **57**, 6181 (1998); *Phys. Rev. D* **57**, 7292 (1998).
7. S. Bonazzola, E.ourgoulhon and J.-A. Marck, *Phys. Rev. Lett.* **82**, 892 (1999)
8. J. A. Font, M. Miller, W. Suen and M. Tobias, submitted (also gr-qc/9811015).
9. M. Shibata, submitted (1999).
10. R. Arnowitt, S. Deser and C. W. Misner, in *Gravitation: An Introduction to Current Research*, edited by L. Witten (Wiley, New York, 1962).
11. See article by J. Winicour in this Volume.
12. A. M. Abrahams *et. al.* (The Binary Black Hole Grand Challenge Alliance) *Phys. Rev. Lett.* **80**, 1812 (1998).
13. M. Shibata and T. Nakamura, *Phys. Rev. D* **52**, 5428 (1995).
14. For example: J. M. Bardeen and T. Piran, *Phys. Rep.* **96**, 205 (1983); C. R. Evans, PhD thesis, University of Texas at Austin (1984); A. M. Abrahams and C. R. Evans, *Phys. Rev. D* **37**, 318 (1988); A. M. Abrahams, G. B. Cook, S. L. Shapiro and S. A. Teukolsky, *Phys. Rev. D* **49**, 5153 (1994).
15. T. W. Baumgarte and S. L. Shapiro, *Phys. Rev. D* **59**, 024007 (1999).
16. A. Lichnerowicz, *J. Math. Pure Appl.* **23**, 37 (1944); J. W. York, Jr., *Phys. Rev. Lett.* **26**, 1656 (1971).
17. T. Nakamura, K. Oohara and Y. Kojima, *Prog. Theor. Phys. Suppl.* **90**, 76 (1987).
18. T. De Donder, *La gravifique einsteinienne* (Gauthier-Villars, Paris, 1921); C. Lanczos, *Phys. Z.* **23**, 537 (1922).
19. S. Frittelli and O. Reula, submitted (1999) (also gr-qc/9904048).
20. Miguel Alcubierre *et.al*, submitted (1999) (also gr-qc/9904013).
21. T. W. Baumgarte, S. A. Hughes and S. L. Shapiro, *Phys. Rev. D*, in press.
22. M. Shibata, T. W. Baumgarte and S. L. Shapiro, *Phys. Rev. D* **58**, 023002 (1998).
23. J. F. Hawley, L. L. Smarr and J. R. Wilson, *Astrophys. J. Suppl.* **55**, 211 (1984).